EFFECT OF RADIATION ON THE FLOW STRUCTURE AND HEAT TRANSFER IN A 2-D GRAY MEDIUM

by

Nesrine RACHEDI[a], Madiha BOUAFIA[b], Messaoud GUELLAL[a*], and Saber HAMIMID[a]

[a] Laboratory of Process Engineering, University Ferhat Abbas Setif-1, Setif, Algeria
[b] Evry Mecanichal and Energy Laboratory – [LMEE], University of Evry, Evry Cedex, France

Original scientific paper
https://doi.org/10.2298/TSCI180108117R

A numerical study of combined natural convection and radiation in a square cavity filled with a gray non-scattering semi-transparent fluid is conducted. The horizontal walls are adiabatic and the vertical are differentially heated. Convection is treated by the finite volumes approach and the discrete ordinates method is used to solve radiative transfer equation using S6 order of angular quadrature. Representative results illustrating the effects of the Rayleigh number, the optical thickness and the Planck number on the flow and temperature distribution are reported. In addition, the results in terms of the average Nusselt number obtained for various parametric conditions show that radiation modifies significantly the thermal behavior of the fluid within the enclosure.

Key words: *natural convection; volumetric radiation, Planck number, optical thickness, semi-transparent medium*

Introduction

The study of combined natural convection radiation in 2-D semi-transparent medium is widely encountered in engineering and remains a topical subject for scientists and researchers in various fields such as furnace design, heat exchangers, cooling of electronic components, nuclear reactors, *etc.* A fair amount of research in this area was devoted to the heat transfer in semi-transparent media. Lauriat [1] studied natural convection in the presence of radiation by considering a gray gas contained in a vertical 2-D cavity of elongation between 5 and 20. P1anck approximation of spherical harmonics method was used for the radiative problem. The same problem was modeled by Yucel *et al.* [2] using the discrete ordinates method. The investigation involves a square cavity whose four walls are black. The Rayleigh number was fixed at 5×10^6 and the variation of the optical thickness was taken into account. Draoui *et al.* [3] studied the Rayleigh number effect using P1anck approximation of spherical harmonics method. The emissivity is equal to 0 for adiabatic walls and 1 for isothermal walls. Colomer *et al.* [4] also addressed combined natural convection and radiation considering both transparent and participating media in a 3-D differentially heated cavity. They solved the radiative transfer equation (RTE) using the discrete ordinates method (DOM) and conservation equations of natural convection by means of segregated SIMPLE like algorithm. In his work, A. Ibrahim [5] was interested in the impact of radiation on the

* Corresponding author, e-mail: mguellal@univ-setif.dz

natural convection in a square cavity filled with binary gaseous mixture where at least one component radiates in the infrared. Laouar-Meftah *et al.* [6] studied the effects of non-gray gas radiation on laminar double diffusive convection in a square cavity filled with air-CO_2 mixtures when vertical walls are maintained at different temperatures and concentrations. Moufekkir *et al.* [7] used hybrid thermal lattice Boltzmann method to study numerically natural convection and volumetric radiation in an isotropic scattering medium within a heated square cavity. Momentum and energy equations are solved by finite difference method, while S8 quadrature of the DOM has been used to solve the RTE. Chaabane *et al.* [8] developed an algorithm for solving natural convection coupled to radiation in a 2-D cavity containing an absorbing, emitting and diffusing medium. The RTE is solved using control volume finite element method: the density, velocity and temperature fields are determined using the two double population Lattice Boltzmann equation.

Kolsi *et al.* [9] studied the effect of radiation and aspect ratio on 3-D natural convection of the $LiNbO_3$ in vertically lengthened enclosures for, Ra = 10^5 and for various optical properties. The conservation equations, expressed according to the vorticity-stream function formulation, and the RTE are resolved by volume control method and the FTn finite volume method, respectively. The obtained numerical results showed that the radiation-conduction parameter affects considerably the principal flow structure.

Other works dealing with combined natural convection-surface radiation in differentially heated cavities have received considerable attention in the literature, either in the case of Boussinesq approximation [10-13] or under Low Mach Number conditions [14, 15].

The purpose of this work is to study the effects of volumetric radiation on the flow and heat transfer of a gray non-scattering semi-transparent fluid within a differentially heated square cavity. A parametric study of impact of main variables involved in the phenomenon will be also conducted.

Physical model and governing equations

Governing equations

The studied physical system is illustrated in fig. 1. It is a square cavity filled with a semi-transparent medium assumed to be homogeneous, incompressible, laminar, gray and non-scattering. The two vertical walls are black ($\varepsilon_{1,2}=1$) and maintained at different temperatures T_C and T_H ($T_C < T_H$), while the two horizontal walls are reflective ($\varepsilon_{3,4}=0$) and perfectly insulated. It will be further assumed that the temperature differences in the flow domain under consideration are small enough to justify the employment of the Boussinesq approximation. The medium is initially at rest and at a uniform temperature $T_0=(T_H+T_C)/2$.

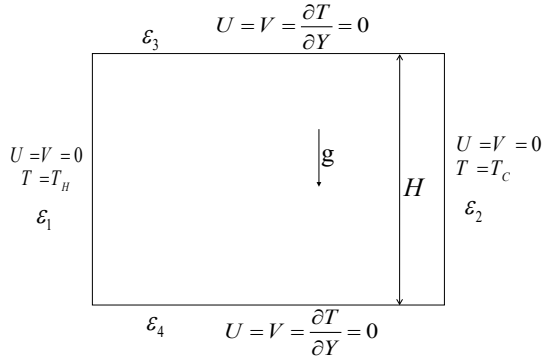

Figure 1. Physical geometry and boundary conditions

The equations to be solved are based on the balance laws of mass, momentum and energy, as well as the RTE which provides the term of radiative source to be inserted into the energy equation.

Theses equations are converted into the non-dimensional form by using the non-dimensional variables:

$$X=\frac{x}{H},\ Y=\frac{y}{H},\ t=\frac{t'V_0}{H},\ U=\frac{u}{V_0},\ V=\frac{v}{V_0},\ V_0=\frac{\nu}{H}\sqrt{\mathrm{Ra}},\ T=\frac{T'-T_0}{\Delta T}$$

$$L=\frac{L'}{4\sigma T_0^4},\ P=\frac{P'}{\rho V_0^2},\ Q_r=\frac{q_r}{4\sigma T_0^4},\ Q_{\mathrm{inc}}=\frac{q_{\mathrm{inc}}}{4\sigma T_0^4},\ \theta_0=\frac{T_0}{\Delta T},\ \Delta T=T_H-T_C$$

Considering the previous assumptions, the governing equations for an unsteady 2-D problem can be written in dimensionless form:

$$\frac{\partial U}{\partial X}+\frac{\partial V}{\partial Y}=0 \tag{1}$$

$$\frac{\partial U}{\partial t}+U\frac{\partial U}{\partial X}+V\frac{\partial U}{\partial Y}=-\frac{\partial P}{\partial X}+\frac{1}{\sqrt{\mathrm{Ra}}}\left(\frac{\partial^2 U}{\partial X^2}+\frac{\partial^2 U}{\partial Y^2}\right) \tag{2}$$

$$\frac{\partial V}{\partial t}+U\frac{\partial V}{\partial X}+V\frac{\partial V}{\partial Y}=-\frac{\partial P}{\partial Y}+\frac{1}{\sqrt{\mathrm{Ra}}}\left(\frac{\partial^2 V}{\partial X^2}+\frac{\partial^2 V}{\partial Y^2}\right)+\frac{1}{\mathrm{Pr}}T \tag{3}$$

$$\frac{\partial T}{\partial t}+U\frac{\partial T}{\partial X}+V\frac{\partial T}{\partial Y}=\frac{1}{\mathrm{Pr}\sqrt{\mathrm{Ra}}}\left(\frac{\partial^2 T}{\partial X^2}+\frac{\partial^2 T}{\partial Y^2}\right)-\frac{1}{\mathrm{Pr}\sqrt{\mathrm{Ra}}}\frac{\theta_0}{\mathrm{Pl}}\vec{\nabla}Q_r \tag{4}$$

with Prandtl number $\mathrm{Pr}=\nu/\alpha$ and Rayleigh number $\mathrm{Ra}=\mathrm{g}\beta\Delta TH^3/\nu\alpha$

The source term in the energy equation is equal to the divergence of the radiative heat flux representing the radiative exchange rate in the cavity which is calculated by the following equations:

$$\mu\left(\frac{\partial L}{\partial X}\right)+\eta\left(\frac{\partial L}{\partial Y}\right)+\tau L=\frac{\tau}{4\pi}\left(1+\frac{T}{\theta_0}\right)^4 \tag{5}$$

$$\vec{\nabla}Q_r=\tau\left[\left(1+\frac{T}{\theta_0}\right)^4-\int_{4\pi}L\mathrm{d}\Omega\right] \tag{6}$$

where Pl is the Planck number defined as $\mathrm{Pl}=k/4H\sigma T_0^3$.

Equation (5) represents the RTE for a 2-D absorbing, emitting and non-scattering medium.

The $L(X,Y,\vec{\Omega})$ is the dimensionless radiation intensity at position (X, Y) in the direction $\vec{\Omega}=\mu\vec{i}+\eta\vec{j}$.

Boundary conditions

The boundary conditions applied on the horizontal walls are described by the equations:

$$U=V=0,\ -\frac{\partial T}{\partial Y}+\varepsilon_3\frac{\theta_0}{\mathrm{Pl}}\left[\frac{1}{4}\left(1+\frac{T}{\theta_0}\right)^4-Q_{\mathrm{inc}}\right]=0 \quad \text{at} \quad Y=0 \quad \text{and for} \quad 0\le \mathrm{X}\le 1 \tag{7}$$

$$U=V=0,\ \frac{\partial T}{\partial Y}+\varepsilon_4\frac{\theta_0}{\mathrm{Pl}}\left[\frac{1}{4}\left(1+\frac{T}{\theta_0}\right)^4-Q_{\mathrm{inc}}\right]=0 \ \text{at} \ Y=1 \ \text{and for} \ 0\le \mathrm{X}\le 1 \tag{8}$$

The Q_{inc} is the incident radiation flux obtained:

$$Q_{\text{inc}}(X,0)=\sum_{\eta_m<0}|\eta_m|\omega_m L(X,0) \quad \text{at} \quad Y=0 \tag{9}$$

$$Q_{\text{inc}}(X,1)=\sum_{\eta_m>0}|\eta_m|\omega_m L(X,1) \quad \text{at} \quad Y=1 \tag{10}$$

In this investigation, adiabatic horizontal walls are completely reflective ($\varepsilon_3 = \varepsilon_4 = 0$). The adiabacity condition is reduced to:

$$-\frac{\partial T}{\partial Y}=0 \quad \text{at} \quad Y=0 \quad \text{for} \quad 0\le X\le 1 \tag{11}$$

$$\frac{\partial T}{\partial Y}=0 \quad \text{at} \quad Y=1 \quad \text{for} \quad 0\le X\le 1 \tag{12}$$

The boundary conditions on the vertical walls are:

$$U=V=0, \quad T=T_{\text{H}} \quad \text{at} \quad X=0 \quad \text{and for} \quad 0\le Y\le 1 \tag{13}$$

$$U=V=0, \quad T=T_{\text{C}} \quad \text{at} \quad X=1 \quad \text{and for} \quad 0\le Y\le 1 \tag{14}$$

The radiative boundary conditions are:

$$L(X,0)=\frac{\varepsilon_3}{4\pi}\left[1+\frac{T(X,0)}{\theta_0}\right]^4+\frac{1-\varepsilon_3}{\pi}Q_{\text{inc}}(X,0) \quad \text{at} \quad Y=0 \quad \text{and for} \quad \eta<0 \tag{15}$$

$$L(X,1)=\frac{\varepsilon_4}{4\pi}\left[1+\frac{T(X,1)}{\theta_0}\right]^4+\frac{1-\varepsilon_4}{\pi}Q_{\text{inc}}(X,1) \quad \text{at} \quad Y=1 \quad \text{and for} \quad \eta>0 \tag{16}$$

$$L(0,Y)=\frac{\varepsilon_1}{4\pi}\left[1+\frac{T(0,Y)}{\theta_0}\right]^4+\frac{1-\varepsilon_1}{\pi}Q_{\text{inc}}(0,Y) \quad \text{at} \quad X=0 \quad \text{and for} \quad \mu<0 \tag{17}$$

$$L(1,Y)=\frac{\varepsilon_2}{4\pi}\left[1+\frac{T(1,Y)}{\theta_0}\right]^4+\frac{1-\varepsilon_2}{\pi}Q_{\text{inc}}(1,Y) \quad \text{at} \quad X=1 \quad \text{and for} \quad \mu>0 \tag{18}$$

with

$$Q_{\text{inc}}(0,Y)=\sum_{\mu_m<0}|\mu_m|\omega_m L(0,Y) \quad \text{at} \quad X=0 \tag{19}$$

$$Q_{\text{inc}}(1,Y)=\sum_{\mu_m>0}|\mu_m|\omega_m L(1,Y) \quad \text{at} \quad X=1 \tag{20}$$

One obtains for vertical walls ($\varepsilon_1 = \varepsilon_2 = 1$):

$$L(0,Y)=\frac{1}{4\pi}\left[1+\frac{T(0,Y)}{\theta_0}\right]^4 \quad \text{at} \quad X=0 \tag{21}$$

$$L(1,Y)=\frac{1}{4\pi}\left[1+\frac{T(1,Y)}{\theta_0}\right]^4 \quad \text{at} \quad \text{X} = 1 \tag{22}$$

And for horizontal walls ($\varepsilon_3 = \varepsilon_4 = 0$):

$$L(X,0)=\frac{1}{\pi}Q_{\text{inc}}(X,0) \quad \text{at} \quad Y=0 \quad \text{and for} \quad \eta<0 \tag{23}$$

$$L(X,1)=\frac{1}{\pi}Q_{\text{inc}}(X,1) \quad \text{at} \quad Y=1 \quad \text{and for} \quad \eta>0 \tag{24}$$

Heat transfer

The average non-dimensional heat transfer rate in terms of convective and radiative Nusselt numbers, are, respectively, defined:

$$\text{Nu}_{cv}=\int_0^1 -\left(\frac{\partial T}{\partial X}\right)_{X=0,1} \text{d}Y \tag{25}$$

$$\text{Nu}_r=\frac{\theta_0}{\text{Pl}}\int_0^1\left[\frac{1}{4}\left(1+\frac{T}{\theta_0}\right)^4-Q_{\text{inc}}\right]_{X=0,1}\text{d}Y \tag{26}$$

The summation of the previous expressions gives the following expression for the global averaged Nusselt number:

$$\text{Nu}_t=\text{Nu}_{cv}+\text{Nu}_r \tag{27}$$

Numerical procedure

The numerical solution of the governing differential eqs. (1)-(4) is obtained by a finite volume technique using staggered arrangement. The discretization in time is done by a second-order backward Euler scheme in which the diffusive and viscous linear terms are implicitly treated while the convective non-linear terms are explicitly treated using an Adams-Bashforth extrapolation. The spatial discretization is based on a non-uniform grid refined in the vicinity of the vertical walls. A technique derived from the classical projection method is employed to solve the coupling between pressure and velocity. The Poisson equations for the pressure correction in the projection method are solved by standard multigrid techniques [15].

The numerical resolution of RTE (5) for a given direction Ω_m is performed using the discrete ordinates method DOM [16]:

$$\mu_m\frac{\partial L_m}{\partial X}+\eta_m\frac{\partial L_m}{\partial Y}+\tau L_m=\tau L_b \tag{28}$$

with $L_b=\sigma T^4/\pi$

The integration of the RTE (28) on control volume $\Delta V=\Delta X\,\Delta Y$ gives:

$$\mu_m\Delta Y(L_{m,\text{E}}-L_{m,\text{W}})+\eta_m\Delta X(L_{m,\text{N}}-L_{m,\text{S}})+\tau\Delta V L_{m,P}=\tau\Delta V L_b \tag{29}$$

where μ_m and η_m are the direction cosines in X- and Y-directions, repectively.

The $L_{m,P}$, $L_{m,\text{E}}$, $L_{m,\text{W}}$, $L_{m,\text{N}}$, $L_{m,\text{S}}$ represent the radiation intensity at the center P and in the four directions (east, west, north, south), respectively. Radiation intensities are known on faces W and S and unknown at the center (P) and on faces E and N.

Two interpolation relationships are needed to eliminate $L_{m,\text{E}}$ and $L_{m,\text{W}}$, thereby allowing to calculate $L_{m,P}$. They are expressed:

$$L_{m,P}=L_{m,\text{W}}+a(L_{m,\text{E}}-L_{m,\text{W}})=L_{m,\text{S}}+b(L_{m,\text{N}}-L_{m,\text{S}}) \tag{30}$$

Coefficients a and b take values 0.5 or 1 according to the scheme type: $a = b = 0.5$ for diamond scheme and $a = b = 1$ for step scheme.

Equation (29) becomes then:

$$L_P = \frac{\left(\frac{\mu_m \Delta X}{a}\right) L_W + \left(\frac{\eta_m \Delta Y}{b}\right) L_S + \tau \Delta V L_b}{\left(\frac{\mu_m \Delta X}{a}\right) + \left(\frac{\eta_m \Delta Y}{b}\right) + \tau \Delta V} \tag{31}$$

The step scheme was used in the present work. The coupling between the convection and radiation is ensured by the divergence of the radiative heat flux. This term source is proportional to the fourth power of the temperature. The solution of this type of problem, guaranteeing the convergence of the computation process, requires the linearization of the temperature using the Taylor series.

Grid independence study is performed to analyse the influence of the grid size on the computational results. Table 1 shows the average total and radiative Nusselt numbers according to the number of mesh nodes, for Pr = 0.71, Ra = $5 \cdot 10^6$, $\tau = 1$, Pl = 0.1, and $\theta_0 = 1.5$. It appears that the solution becomes independent of grid size at 161×161.

Table 1. Grid size effect on the average Nusselt number (total and radiative)

	33×33	57×57	97×97	129×129	161×161	257×257
Nu_t	13.32	13.32	12.98	12.96	12.58	12.58
Nu_r	4.563	4.4561	4.481	4.470	4.2	4.3

Results and discussions

In order to verify the developed numerical code, a comparison of our results with the literature was performed, by considering the total Nusselt number along the hot wall. Calculations were carried out for Pr = 0.71, Ra = $5 \cdot 10^6$, $\tau = 1$, and $\theta_0 = 1.5$. Table 2 shows a good agreement with results of Moufekkir *et al.* [7].

It is interesting to note that laminar flow assumption was adopted by several previous studies working in the same conditions: Ra = $5 \cdot 10^6$, Pr = 0.71 [2, 5-7].

Table 2. Total Nusselt number on the hot wall (Pr = 0.71, Ra = 5.10^6, $\tau = 1$ and $\theta_0 = 1.5$)

Pl	Present study (uniform grid)	Present study (non-uniform grid)	[7] (uniform grid)
0.1	12.58	12.01	12.069
1	7.800	7.752	7.729
10	7.273	7.226	7.314
100	7.258	7.253	7.273

To analyze the effects of the Planck number, the optical thickness, τ, and the Rayleigh number, on the heat transfer and fluid-flow in in steady--state conditions, we consider the following parameters: Pr = 0.71, Pl = 0.1....100, τ = = 0....5, Ra = 10^4..10^6, and $\theta_0 = 1.5$.

The condition of stability is verified by examining the time evolution of temperature and velocity fluid for Pl = 0.02, $\tau = 1$, and Ra = 5.10^6, fig. 2. The results obtained in unsteady state revealed that there is a great fluctuation at the beginning of the regime, and the transition to the steady state occurs beyond a time of 50, from which the flow becomes stable.

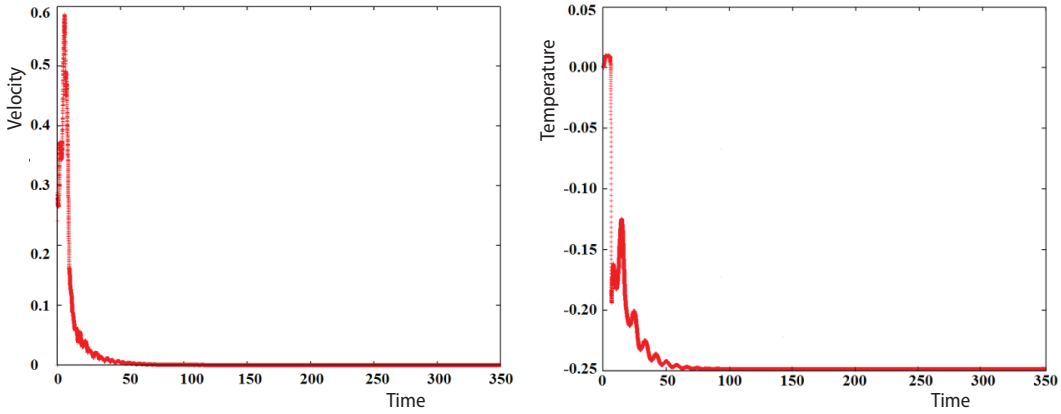

Figure 2. Variation of fluid temperature and velocity *vs.* time

Effect of Planck number

The fixed parameters of simulation are Ra = $5 \cdot 10^6$, $\tau = 1$. However, to examine the impact of the Planck number, we consider different values of Planck number varying from 0.1 to 100. At low Planck number (Pl = 0.1), the streamlines have a two-cell shape indicating a two asymmetrical secondary flows. With increasing Planck number, cells are decomposed into S-shape indicating a unicellular flow in the core of the cavity, fig. 3. The flow and temperature fields present symmetrical structure with respect to the cavity center, indicating therefore a similar behavior of the fluid when the heat transfer is governed by pure natural convection.

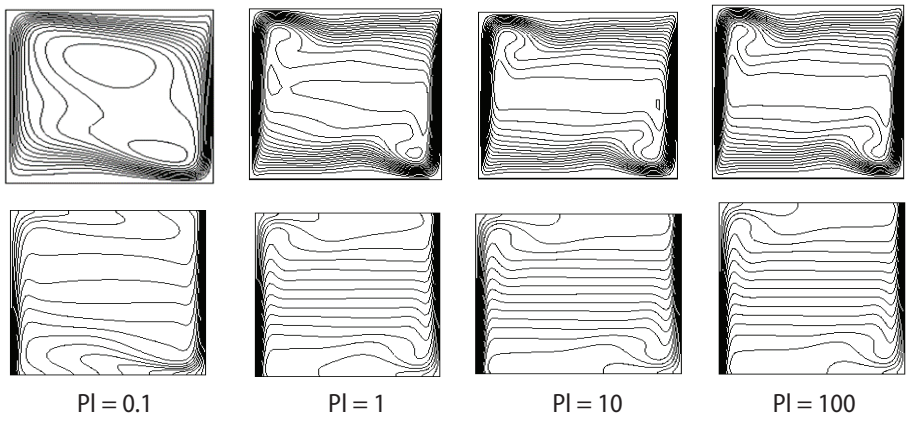

Figure 3. Streamlines (top) and temperature contours (bottom)

The influence of the Planck number on the temperature and velocities is highlighted in figs. 4 and 5. It is observed that the decrease in the Planck number causes an intensification of the temperature and velocity gradients near the active walls. Profiles show that the Planck number increases the stratification in the cavity core, fig. 4, and reduces the amplitude of horizontal velocity, fig. 5.

Figure 6 illustrates the variation of average total and radiative Nusselt numbers on the hot wall for different values of Planck number. It is worth noting that the Planck number, also known as conduction-radiation parameter, expresses the ratio of conduction to radiation effects.

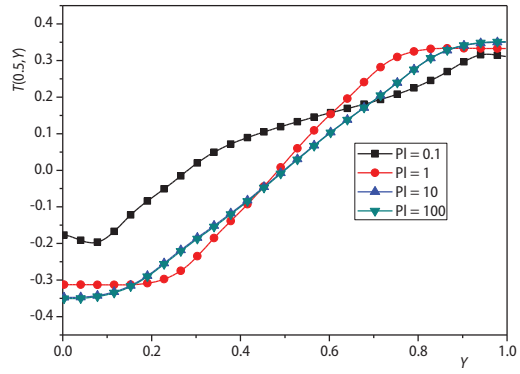

Figure 4. Cross-section of the temperature at mid-plane cavity $X = 0.5$

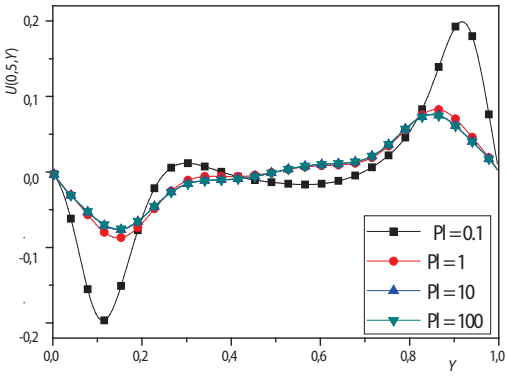

Figure 5. Horizontal velocity at the vertical cross-section $X = 0.5$

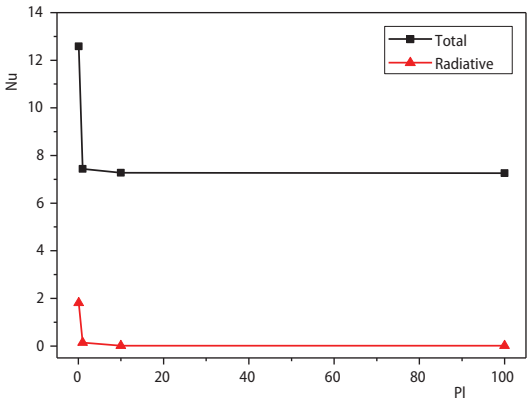

Figure 6. Variations of the average total and radiative Nusselt numbers as a function of Planck number

We can note that the increase in the values of Planck number, leads to decrease in the average total Nusselt number. The same behavior is observed for the average radiative Nusselt number. Heat transfer is dominated by radiation when the Planck number is low.

Effect of the optical thickness

The effect of the optical thickness, τ, on temperature contours and streamlines is displayed in fig. 7. A strong deformation on the temperature distribution is observed when τ increases. For low values of the optical thickness, a re-circulation flow appears near the horizontal boundary layers. However, the re-circulation movements on the vicinity of the cavity walls tend to disappear with increasing the optical thickness. A large temperature gradient is noticed near to the boundary-layer of cold wall. This is can be explained by the fact that the medium is more opaque and the radiation effect is stronger. We can note that the

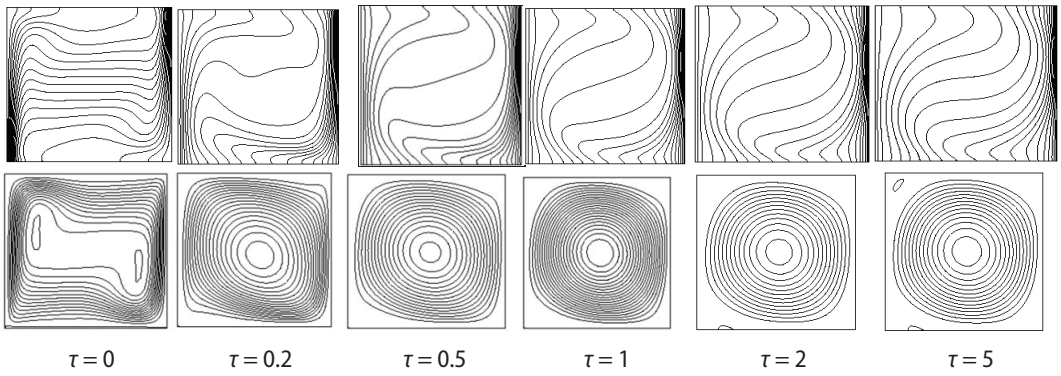

Figure 7. Temperature contours (top) and streamlines (bottom)

symmetrical nature of the flow is strongly broken in the presence of radiation.

Figure 8 shows the variation of average total Nusselt number on the hot wall according to the optical thickness, τ. With increasing of the optical thickness, the Nusselt number decreases indicating a significant heat exchange for a thicker medium. Figures 9 and 10 illustrate the variations of temperature as a function of optical thickness, τ. Temperature profiles at mid-plane and mid-height cavity are greatly influenced by the radiation. It can be seen for a large optical thickness ($\tau > 0.5$), temperature profiles depend slightly on τ.

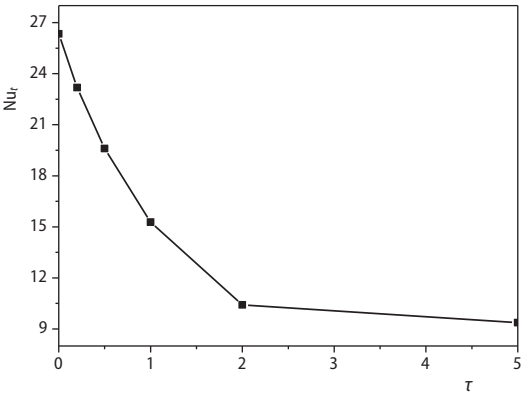

Figure 8. Variations of the average total Nusselt number as a function of optical thickness

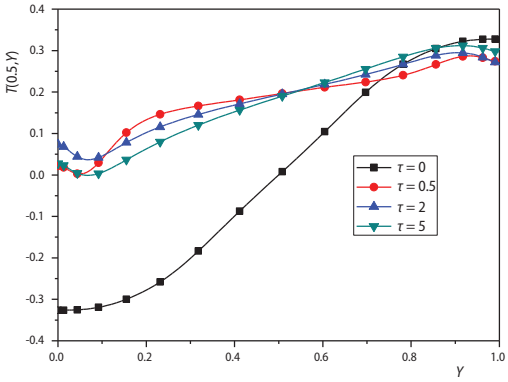

Figure 9. Cross-section of the temperature at mid-plane cavity for Ra = $5 \cdot 10^6$ and Pl = 0.02

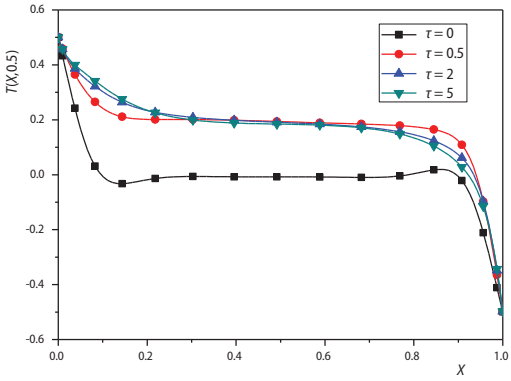

Figure 10. Cross-section of the temperature at mid-height cavity for Ra = $5 \cdot 10^6$ and Pl = 0.02

Analysis of figs. 11 and 12 shows that the maximum values of the horizontal and vertical velocities are strongly influenced by the optical thickness. An increase in the maximum velocity values can also be seen when τ increases.

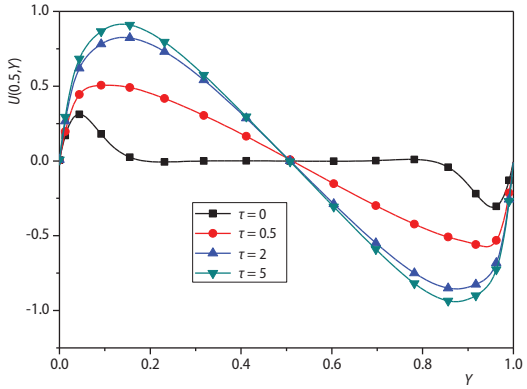

Figure 11. Horizontal velocity at the vertical cross-section for Ra = $5 \cdot 10^6$ and Pl = 0.02

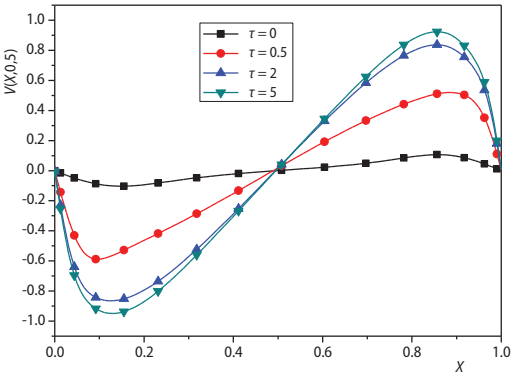

Figure 12. Vertical velocity at the horizontal cross-section for Ra = $5 \cdot 10^6$ and Pl = 0.02

Effect of Rayleigh number

Another aim of this study is to examine the effect of Rayleigh number on the flow and heat transfer in presence of radiation ($\tau = 1$). Computations are carried out for different values of Rayleigh number ($10^3 \leq Ra \leq 10^6$) and Pl = 0.02. Results obtained in terms of streamlines and isotherms are plotted in fig. 13. For low values of Rayleigh number, intensity of circulation is low, streamlines are circular, and isotherms tend to be parallel to active walls because heat transfer is done by conduction. Aside from a slight reduction in re-circulation intensity at the core of the cavity, the effect of radiation on streamlines is not significant. The reduction of temperature gradients gives an indication of the importance of the radiative flux. For a large Rayleigh number, the isotherms move in a counterclockwise direction and become almost horizontal in the cavity core. The temperature contours show the increase of temperature gradient near cold wall due to the radiative exchange. At the core region, the presence of radiation leads to a homogenization of the temperature within the cavity.

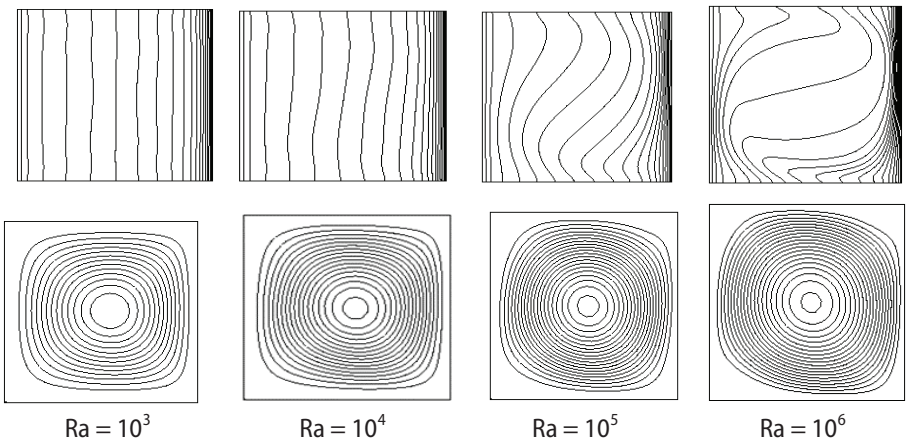

Figure 13. Isotherms (top) and streamlines (bottom) as a function of Ra for Pl = 0.02

As shown in fig. 14, the results in term of heat exchange reveal that the Nusselt number increases with increasing Rayleigh number and decreases with the augmentation of the optical thickness.

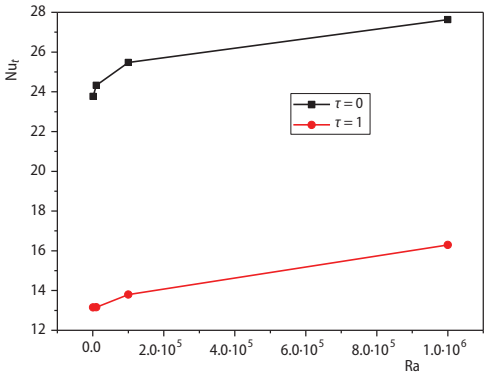

Figure 14. Variation of average total Nusselt number on the hot wall as a function of Rayleigh number

Velocity components are plotted in fig. 15 across the mid-planes. Unlike the case of low Rayleigh values, the flow velocity becomes large when Rayleigh number increases and the circulation becomes strong near the vertical walls. Due to the presence of radiation, the temperature and velocities profiles are no longer symmetric and the fluid is less stratified at the center region of the cavity, figs. 15 and 16.

Conclusions

In the present paper, computations have been carried out to study the combined natural convection and volumetric radiation in a differ-

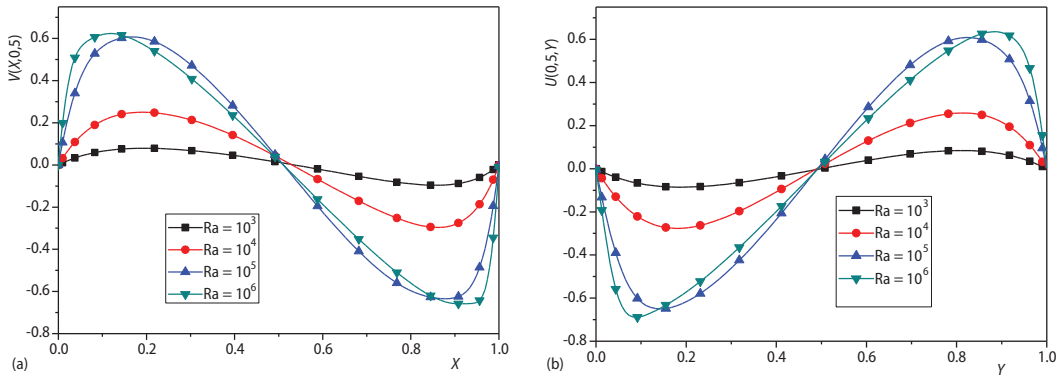

Figure 15. Profiles of vertical (a) and horizontal (b) velocities across the mid-planes for different Rayleigh numbers, Pl = 0.02 and $\tau = 1$

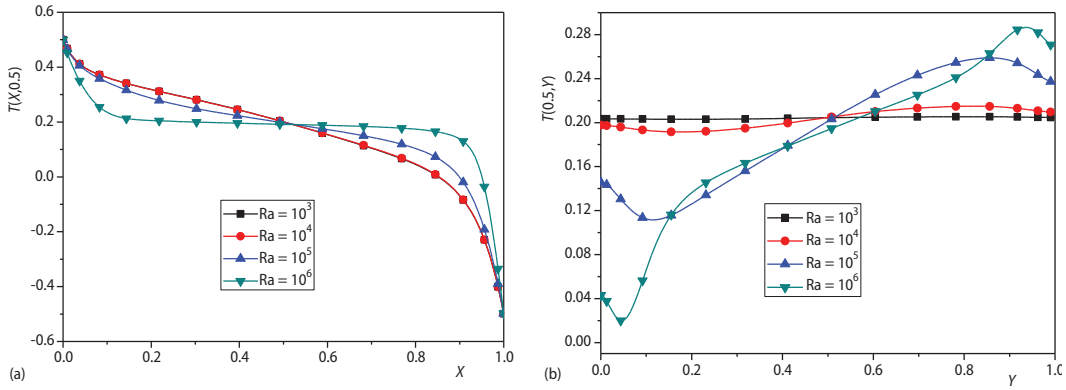

Figure 16. Temperature profiles at mid-height (a) and mid-plane (b) for different values of Rayleigh number and Pl = 0.02

entially-heated cavity filled with a gray non-scattering semi-transparent medium. In the presence of radiation, isotherms and streamlines are strongly affected and velocities are intensified particularly for large Rayleigh number. The study shows that in radiatively thin media, multicellular structures can appear within the cavity. The decrease in the value of Planck number leads to an intensification of the temperature and velocity gradients near the active walls. It is also noted that the Planck number increases the stratification in the cavity core and reduces the velocity amplitude.

Nomenclature

C_p – specific heat capacity, [Jkg^{-1}K^{-1}]
g – gravitational acceleration, [ms^{-2}]
H – dimension of the enclosure, [m]
k – thermal conductivity, [Wm^{-1}K^{-1}]
L_b – radiation intensity of the black body, [Wm^{-2}]
L – dimensionless radiation intensity, [–]
Nu – average Nusselt number, [–]
Pl – Planck number, ($=k/4H\sigma T_0^3$), [–]
Pr – Prandtl number ($=\nu/\alpha$), [–]
P – dimensionless pressure, [–]
Q_{inc} – dimensionless incident radiative flux, [–]
Q_r – dimensionless radiative heat flux, [–]
q_r – radiative heat flux, [Wm^{-2}]
Ra – Rayleigh number ($=g\beta\Delta TH^3/\nu\alpha$), [–]
T – dimensionless temperature, [–]
t – dimensionless time, [–]
U, V – dimensionless velocity-component, [–]
u, v – dimensional velocity-components, [ms^{-1}]
X, Y – dimensionless co-ordinates, [–]
x, y – Cartesian co-ordinates, [m]

Greeksymbols

α – thermal diffusivity, $(=k/\rho C_p)$, [ms^{-1}]
β – thermal expansion coefficient, [K^{-1}]
ε – emissivity, [–]
κ – absorption coefficient, [m^{-1}]
ν – kinematic viscosity, [m^{2}s^{-1}]
ρ – fluiddensity, [kgm^{-3}]
σ – Stefan-Boltzmann constant, [Wm^{-1}K^{-1}]
μ, η – direction cosines
ω_m – weight in the direction Ω_m
τ – optical thickness, $(=H\kappa)$
θ_0 – dimensionless reference temperature, $[=T_0/(T_H - T_C)]$, [–]

Subscripts

‘ – dimensional variables
cv – convective
0 – reference state
C – cold
H – hot
r – radiative
t – total

References

[1] Lauriat, G., Combined Radiation-Convection in Gray Fluids Enclosed in Vertical Cavities, *J. Heat Transfer*, *104* (1982), 4, pp. 609-615
[2] Yucel, A., *et. al.*, Natural Convection and Radiation in a Square Enclosure, *Numer. Heat Transfer A-Appl.*, *15* (1989), 2, pp. 261-278
[3] Draoui, A., *et al.*, Numerical Analysis of Heat Transfer by Natural Convection and Radiation in Participating Fluids Enclosed in Square Cavities, *Numer. Heat Transfer A-Appl.*, *20* (1991), 2, pp. 253-261
[4] Colomer, G., *et al.*, Three-Dimensional Numerical Simulation of Convection and Radiation in a Differentially Heated Cavity Using the Discrete Ordinates Method, *Int. J. Heat Mass Transfer*, *47* (2004), 2, pp. 257-269
[5] Ibrahim, A., Coupling of Natural Convection and Radiation in Absorbing-Emitting Gas Mixtures (in French), Ph. D. thesis, University of Poitiers, Poitiers, France, 2010
[6] Laouar-Meftah, S., *et al.*, Comparative Study of Radiative Effects on Double Diffusive Convection in Non gray Air-CO_2 Mixtures in Cooperating and Opposing Flow, *Math. Probl. Eng.*, *2015* (2015), ID 586913
[7] Moufekkir, F., *et al.*, Numerical Prediction of Heat Transfer by Natural Convection and Radiation in an Enclosure Filled with an Isotropic Scattering Medium, *J. Quant. Spectrosc. Ra*, *113* (2012), 13, pp. 1689-1704
[8] Chaabane, R., *et al.*, Numerical Study of Transient Convection with Volumetric Radiation Using an Hybrid Lattice Boltzmann BGK-Control Volume Finite Element Method, *J. Heat Transfer*, *139* (2017), 9, pp.1-7
[9] Kolsi, L., *et al*., Combined Radiation-Natural Convection in Three-Dimensional Verticals Cavities, *Thermal Science*, *15* (2011), Suppl. 2, pp. S327-S339
[10] Lauriat, G., Desrayaud, G., Effect of Surface Radiation on Conjugate Natural Convection in Partially Open Enclosures, *Int. J. Therm. Sci*., *45* (2006), 4, pp. 335-346
[11] Wang, H., *et al.*, Numerical Study of Natural Convection-Surface Radiation Coupling in Air-Filled Square Cavities, *C. R. Mecanique*, *334* (2006), 1, pp. 48-57
[12] Astanina, M., *et al.*, Effect of Thermal Radiation on Natural Convection in a Square Porous Cavity Filled with a Fluid of Temperature-Dependent Viscosity, *Thermal Science*, *22* (2018), 1B, pp. 391-399
[13] Hamimid, S., Guellal, M., Numerical Analysis of Combined Natural Convection-Internal Heat Generation Source-Surface Radiation, *Thermal Science*, *20* (2016), 6, pp. 1879-1889
[14] Hamimid, S., *et al.*, Numerical Simulation of Combined Natural Convection Surface Radiation for Large Temperature Gradients, *J. Thermophys. Heat Transfer*, *29* (2015), 3, pp.1509-1517
[15] Bouafia, M., *et al.*, Non-Boussinesq Convection in a Square Cavity with Surface Thermal Radiation, *Int. J. Therm. Sci.*, *96* (2015), Oct., pp. 236-247
[16] Modest, M. F., *Radiative Heat Transfer*, 2nd ed., Academic Press, San Diego, Cal., USA, 2003

Paper submitted: January 8, 2018
Paper revised: March 1, 2018
Paper accepted: March 12, 2018